

Article

# Complexes of Formaldehyde and $\alpha$ -Dicarbonyls with Hydroxylamine: FTIR Matrix Isolation and Theoretical Study

Barbara Golec <sup>1,\*</sup> , Magdalena Sałdyka <sup>2</sup> and Zofia Mielke <sup>2</sup><sup>1</sup> Institute of Physical Chemistry, Polish Academy of Sciences, Kasprzaka 44/52, 01-224 Warsaw, Poland<sup>2</sup> Faculty of Chemistry, University of Wrocław, F. Joliot-Curie 14, 50-383 Wrocław, Poland; magdalena.saldyka@chem.uni.wroc.pl (M.S.); zofia.mielke@chem.uni.wroc.pl (Z.M.)

\* Correspondence: bgolec@ichf.edu.pl; Tel.: +48-22-343-3410

**Abstract:** The interactions of formaldehyde (FA), glyoxal (Gly) and methylglyoxal (MGly) with hydroxylamine (HA) isolated in solid argon and nitrogen were studied using FTIR spectroscopy and ab initio methods. The spectra analysis indicates the formation of two types of hydrogen-bonded complexes between carbonyl and hydroxylamine in the studied matrices. The cyclic planar complexes are stabilized by O–H ··· O(C), and C–H ··· N interactions and the nonplanar complexes are stabilized by O–H ··· O(C) bond. Formaldehyde was found to form with hydroxylamine, the cyclic planar complex and methylglyoxal, the nonplanar one in both argon and nitrogen matrices. In turn, glyoxal forms with hydroxylamine the most stable nonplanar complex in solid argon, whereas in solid nitrogen, both types of the complex are formed.

**Keywords:** carbonyls; hydroxylamine; hydrogen bond; matrix isolation; vibrational spectroscopy; computational chemistry



**Citation:** Golec, B.; Sałdyka, M.; Mielke, Z. Complexes of Formaldehyde and  $\alpha$ -Dicarbonyls with Hydroxylamine: FTIR Matrix Isolation and Theoretical Study. *Molecules* **2021**, *26*, 1144. <https://doi.org/10.3390/molecules26041144>

Academic Editors: Rui Fausto, Sylvia Turrell and Gulce Ogruc Ildiz

Received: 26 January 2021  
Accepted: 18 February 2021  
Published: 20 February 2021

**Publisher's Note:** MDPI stays neutral with regard to jurisdictional claims in published maps and institutional affiliations.



**Copyright:** © 2021 by the authors. Licensee MDPI, Basel, Switzerland. This article is an open access article distributed under the terms and conditions of the Creative Commons Attribution (CC BY) license (<https://creativecommons.org/licenses/by/4.0/>).

## 1. Introduction

Chemical and photochemical reactions often proceed through many intermediate stages between the substrates and products. The reactive intermediates formed at the first stages are usually not observed at normal conditions but can be stabilized in an inert environment. The excellent technique for such a purpose is a low-temperature matrix isolation method, which enables the isolation of unstable intermediates in the rare gas matrix [1]. Many reactions begin with the formation of the molecular complexes between the substrates, which also can be isolated in the matrices. Using the FTIR spectroscopy and ab initio methods, we are able to distinguish the nature of interactions and the structures of the isolated complexes [2,3].

In this work, we used the FTIR matrix isolation spectroscopy and MP2 calculations to investigate the structures of the complexes formed between simple carbonyl (formaldehyde) and  $\alpha$ -dicarbonyl compounds glyoxal and methylglyoxal, with hydroxylamine in argon and nitrogen environment. Identification and characterization of these complexes is the first step of our study on isolation of highly unstable intermediate, called hemiaminal, that is formed in oxime formation reaction [4,5] and will be the subject of our next paper. Oximes are widely used compounds in synthetic chemistry in biomedical fields, for example, in the coupling reactions of peptides, proteins, oligosaccharides, and oligonucleotides and in bioconjugation reaction [6–11]. On the other hand, to explain the acid-catalyzed reaction of nucleophiles with the carbonyl group, the formation of weak hydrogen bonds between the carbonyl group of aldehydes and ketones with proton donors has been postulated [12]. Therefore, the deep understanding of the hydrogen bond interaction of carbonyl compounds with nucleophilic hydroxylamine is an important issue.

Some binary complexes between formaldehyde or  $\alpha$ -dicarbonyls and proton donors have been investigated. The most studied are the complexes of formaldehyde with water [13–31]. Additionally, there are some words about the interaction of formaldehyde with

hydrogen halides and cyanide [32–36], formamide [37,38], nitroxyl [39], ammonia [33], methane [40], and methanol [41]. For  $\alpha$ -dicarbonyls, the interactions of glyoxal, methylglyoxal and diacetyl with water [42], methanol [43,44], hydrogen peroxide [45,46], and hydroperoxyl radical [47] have been studied. The results of these investigations show that the water complexes of formaldehyde or  $\alpha$ -dicarbonyls trapped in argon matrices are stabilized by the  $\text{OH}\cdots\text{O}(\text{C})$  hydrogen bond formed between water and carbonyl oxygen. The most stable structure of the methanol complex with formaldehyde is also predicted to be stabilized by a hydrogen bond. However, for the methanol complexes with  $\alpha$ -dicarbonyls, the ab initio calculations predict the non-hydrogen-bonded structures as the most stable ones. Experimental data show that in the Ar matrix, glyoxal forms the non-hydrogen-bonded structure with methanol, but methylglyoxal and diacetyl form the planar cyclic structures stabilized by  $\text{O}-\text{H}\cdots\text{O}(\text{C})$  and  $\text{C}-\text{H}\cdots\text{O}(\text{C})$  interactions.

Hydroxylamine dimers and their complexes with water and ammonia isolated in argon and nitrogen matrices have been studied by Yao and Ford [48–50]. The dimer  $(\text{NH}_2\text{OH})_2$  has a cyclic structure stabilized by two  $\text{O}-\text{H}\cdots\text{N}$  hydrogen bonds. In hydroxylamine complexes with  $\text{H}_2\text{O}$  and  $\text{NH}_3$ , the OH group of  $\text{NH}_2\text{OH}$  acts as a proton donor to the oxygen or nitrogen atom of water or ammonia, respectively. These complexes are relatively strong; the  $\nu(\text{OH})$  band of hydroxylamine shifts by 100 and 300  $\text{cm}^{-1}$  to lower wavenumbers in the spectra of the  $\text{H}_2\text{O}$  and  $\text{NH}_3$  complexes, respectively. A much weaker complex formed between hydroxylamine and carbon monoxide stabilized by  $\text{O}-\text{H}\cdots\text{C}=\text{O}$  interaction has been observed in the Ar matrix. In this complex, the  $\nu(\text{OH})$  band shifts 39  $\text{cm}^{-1}$  towards lower energies [51]. For the isocyanic acid-hydroxylamine complex, only the hydrogen-bonded structure with the NH group of  $\text{HNCO}$  attached to the oxygen atom of the  $\text{NH}_2\text{OH}$  molecule was identified in solid argon [52].

## 2. Results and Discussion

### 2.1. Formaldehyde–hydroxylamine Complexes

Ab Initio Calculations. The MP2/6-311++G(2d,2p) calculations predict the stability of five different structures of a hydrogen-bonded complex between formaldehyde and hydroxylamine with stoichiometry 1:1. Their structures and binding energies ( $\Delta E^{\text{CP}}(\text{ZPE})$  in  $\text{kJ mol}^{-1}$ ) are presented in Figure 1 and Figure S1 in Supplementary Material.

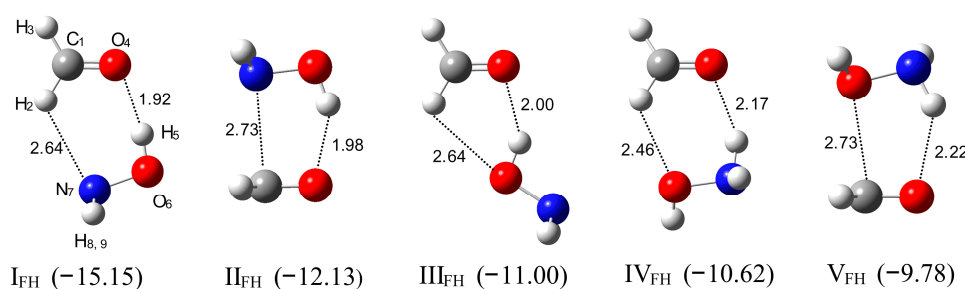


**Figure 1.** The optimized structures of the  $\text{HCHO}-\text{NH}_2\text{OH}$  complexes,  $\text{I}_{\text{FH}}-\text{V}_{\text{FH}}$ . The  $\Delta E_{\text{CP}}(\text{ZPE})$ -binding energies in  $\text{kJ mol}^{-1}$  are given in parentheses. The intermolecular distances are given in Å.

The most stable complex,  $\text{I}_{\text{FH}}$ , has a cyclic structure in which two subunits are stabilized by two hydrogen bonds: the relatively strong  $\text{OH}\cdots\text{O}(\text{C})$  bond ( $R(\text{H}\cdots\text{O}) = 1.92 \text{ \AA}$ ) and the weak  $\text{CH}\cdots\text{N}$  interaction ( $R(\text{H}\cdots\text{N}) = 2.64 \text{ \AA}$ ). The selected structural parameters of this complex are listed in Table S1 in Supplementary Material. In this complex, the OH group of hydroxylamine acts as a proton donor and the nitrogen atom as a proton acceptor. The two hydrogen bonds are positioned in one plane, which is reflected by the value of the torsion angles  $\varphi\text{C1}-\text{O4}-\text{H5}-\text{O6}$  and  $\varphi\text{C1}-\text{H2}-\text{N7}-\text{O6}$  equal to 0 degrees. This structure is about 3  $\text{kJ mol}^{-1}$  more stable than  $\text{II}_{\text{FH}}$ , which is stabilized by one hydrogen bond,  $\text{OH}\cdots\text{O}(\text{C})$ , formed between the OH group of hydroxylamine and the oxygen atom of formaldehyde ( $R(\text{H}\cdots\text{O}) = 1.98 \text{ \AA}$ ). The next three structures,  $\text{III}_{\text{FH}}$ ,  $\text{IV}_{\text{FH}}$  and  $\text{V}_{\text{FH}}$ ,

have comparable energies ( $-11.00$ ,  $-10.62$ , and  $-9.78$  kJ mol $^{-1}$ , respectively). In III<sub>FH</sub>, the hydroxylamine hydroxyl group interacts with formaldehyde forming OH $\cdots$ O(C) bond ( $R\cdots O(C) = 2.0$  Å) weaker than in I<sub>FH</sub> and II<sub>FH</sub>. The structures IV<sub>FH</sub> and V<sub>FH</sub> are stabilized by NH $\cdots$ O(C) interaction between the NH group of hydroxylamine and an oxygen atom of formaldehyde.

**Experimental Spectra.** The infrared spectra of the formaldehyde and hydroxylamine molecules isolated in argon and nitrogen matrices agree with those previously reported [25,48,49,53–56]. When both FA and HA are trapped in the matrices, a set of new absorptions appears in the spectra that are not observed in the spectra of parent molecules. The selected regions of experimental spectra of FA/HA/Ar matrix are shown in Figure 2.

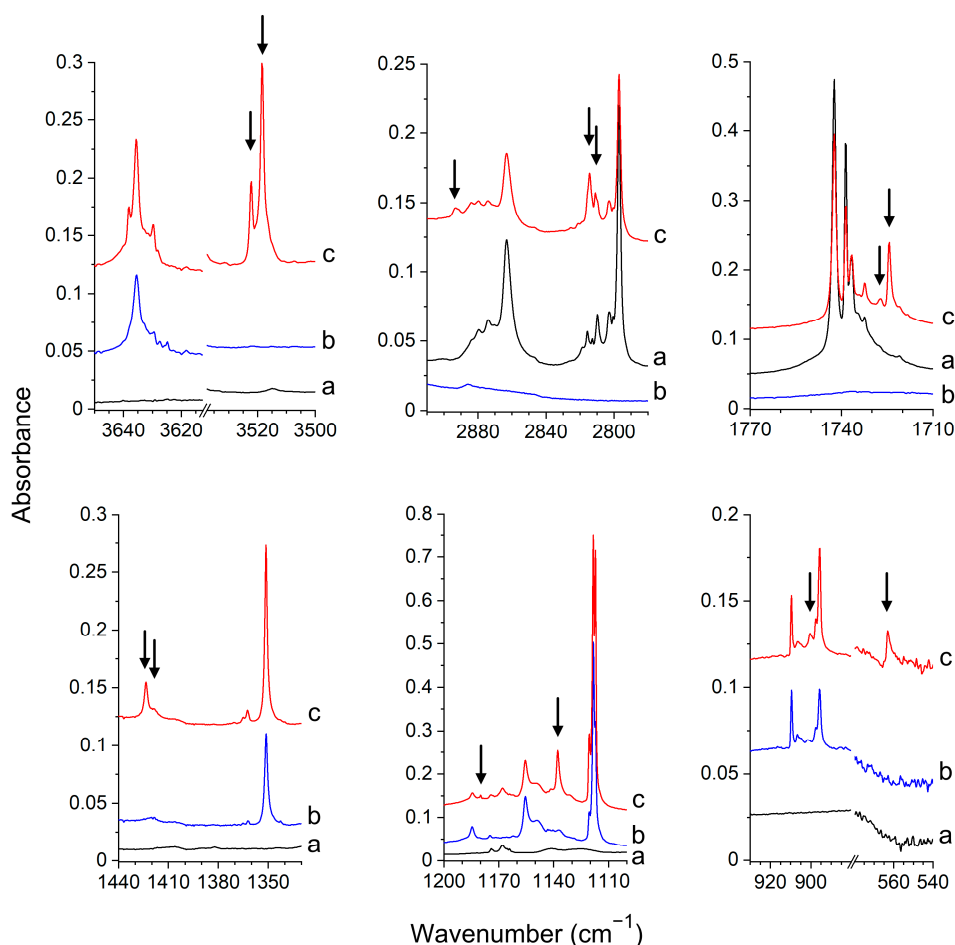


**Figure 2.** The spectra of the HCHO/Ar (a), NH<sub>2</sub>OH/Ar (b) and HCHO/NH<sub>2</sub>OH/Ar (c) matrices recorded after matrix deposition at 11 K. The bands of the HCHO–NH<sub>2</sub>OH complex are marked by the arrows.

The new absorptions, indicated in the spectra by the arrows, are assigned to the HCHO–NH<sub>2</sub>OH complex. The splitting of the bands is assigned to the matrix cage effect as the observed spectral pattern of the complex differs in the spectra of argon and nitrogen matrices. In Table 1, the observed experimental wavenumbers and wavenumbers shifts are compared with the MP2 calculated values predicted for the two most stable forms of the formaldehyde–hydroxylamine complexes (I<sub>FH</sub> and II<sub>FH</sub>). The large red-shift of the  $\nu(\text{OH})$  band of HA ( $-115.1$  and  $-124.6$  cm $^{-1}$  in Ar and N<sub>2</sub> matrices, respectively) and the red-shift of the  $\nu(\text{C}=\text{O})$  band of FA after complex formation ( $-16.8$  and  $-17.1$  cm $^{-1}$ ) in Ar and N<sub>2</sub> matrices, respectively indicate that the complex has the hydrogen-bonded structure with the NH<sub>2</sub>OH molecule attached to the carbonyl group of HCHO. The comparison of the experimental and theoretical spectra clearly shows that in both argon and nitrogen

matrices, one type of complex is formed. The identified complex bands for the OH, C=O groups evidence that the I<sub>FH</sub> structure is created in both matrices. The calculations indicate that for the structure I<sub>FH</sub>, the strongest band corresponds to the  $\nu(\text{OH})$  stretching vibration (408 km mol<sup>-1</sup>). It is ca 3.5 times more intense than the other band of the OH group, namely  $\tau(\text{OH})$  (115 km mol<sup>-1</sup>). For the II<sub>FH</sub> complex, both  $\nu(\text{OH})$  and  $\tau(\text{OH})$  bands are predicted to have comparable intensities (117, 122 km mol<sup>-1</sup>). Moreover,  $\tau(\text{OH})$  is distinctly more perturbed in I<sub>FH</sub> than in II<sub>FH</sub> (+238, +106 cm<sup>-1</sup>, respectively). In experimental spectra, the  $\nu(\text{OH})$  band is much more intense than the  $\tau(\text{OH})$  one, which indicates that the I<sub>FH</sub> structure is formed. The observed shift of the  $\tau(\text{OH})$  vibration of HA (162.1 cm<sup>-1</sup>, Ar; 172.5 cm<sup>-1</sup>, N<sub>2</sub>) also corresponds better with the value +238 cm<sup>-1</sup> predicted for the structure I<sub>FH</sub> than with the value +106 cm<sup>-1</sup> calculated for the complex II<sub>FH</sub>. The other calculated wavenumber shifts and intensities for the I<sub>FH</sub> structure also match well the observed ones, as one can see in Table 1.

**Table 1.** The comparison of the observed wavenumbers (cm<sup>-1</sup>) and wavenumber shifts ( $\Delta\nu = \nu_{\text{FH}} - \nu_{\text{M}}$ ) for the HCHO–NH<sub>2</sub>OH (FH) complexes present in the argon (Ar) and nitrogen (N<sub>2</sub>) matrices with the corresponding values calculated for the structures I<sub>FH</sub> and II<sub>FH</sub>. In parentheses, the calculated band intensities are given (km mol<sup>-1</sup>).

Approximate Description	Experimental						Calculated	
	Ar			N <sub>2</sub>			$\Delta\nu$	
	$\nu_{\text{M}}$	$\nu_{\text{FH}}$	$\Delta\nu^1$	$\nu_{\text{M}}$	$\nu_{\text{FH}}$	$\Delta\nu^1$	I <sub>FH</sub>	II <sub>FH</sub>
<b>Hydroxylamine</b>								
$\nu(\text{OH})$	3635.5	3522.2 3518.5	−115.1	3637.6	3516.0 3510.0	−124.6	−141 (408)	−126 (117)
$\delta(\text{NOH})$	1351.2	1423.4 1418.7	+69.9	1367.4	1427.7	+60.3	+86 (36)	+62 (51)
$\omega(\text{NH}_2)$	1118.3	1137.8	+19.5	1133.0	1156.7	+23.7	+24 (117)	+13 (102)
$\nu(\text{NO})$	895.6	900.5	+4.9	895.3	897.0 901.8	+4.1	+6 (7)	+8 (4)
$\tau(\text{OH})$	402 <sup>2</sup>	562.1	+162.1	402 <sup>2</sup>	574.5	+172.5	+238 (115)	+106 (122)
<b>Formaldehyde</b>								
$\nu_{\text{as}}(\text{CH})$	2864.1	2893.3 2891.1	+28.1	2866.4	2892.3	+25.9	+56 (34)	+34 (72)
$\nu_{\text{s}}(\text{CH})$	2798.0	2814.2 2811.0	+14.6	2800.1 2798.0			+25 (77)	+29 (56)
$\nu(\text{C}=\text{O})$	1742.2	1727.1 1724.4	−16.8	1740.7 1739.7	1723.1	−17.1	−20 (53)	−9 (66)
$\delta(\text{CH}_2)$	1499.1	1493.9	−5.2	1499.6 1496.4			−6 (15)	−3 (14)
$\gamma(\text{CH}_2)$	1168.6	1179.8	+11.2	1170.0 1167.9	1180.0	+11.0	+12 (5)	+8 (20)

<sup>1</sup> In the case when the splitting of the band was observed, the average of the two wavenumbers at which the two peaks appear was taken into account to calculate  $\Delta\nu$  value. <sup>2</sup> Gas-phase data [56].

Nelander [25] studied the HCHO–H<sub>2</sub>O complex and found that the hydrogen-bonded structures stabilized by the O–H···O(C) bond are formed both in argon and nitrogen matrices. The wavenumbers shifts of the H<sub>2</sub>O vibrations for the complex isolated in solid argon were found to be −25.0 cm<sup>-1</sup> for the  $\nu_{\text{as}}(\text{OH})$  and −52.9, −57.6 cm<sup>-1</sup> for the  $\nu_{\text{s}}(\text{OH})$  vibrations, whereas  $\nu(\text{C}=\text{O})$  of FA was shifted by −5.2 cm<sup>-1</sup> after complex formation. Such shifts pattern indicates that the HCHO–H<sub>2</sub>O complex is weaker than the HCHO–NH<sub>2</sub>OH one.

## 2.2. Glyoxal–hydroxylamine Complexes

**Ab Initio Calculations.** Glyoxal in the standard conditions exists in a *trans* form [57–59], so exclusively, this conformer is considered in our study. The MP2 calculations show the stability of eight different complexes of 1:1 stoichiometry, which can be formed between Gly and HA. The four most stable ones are presented in Figure 3, and all complexes are shown in Figure S2 in Supplementary Material. The selected structural parameters of these complexes are listed in Table S2. The two most stable structures, I<sub>GH</sub> and II<sub>GH</sub>, are the nonplanar hydrogen-bonded complexes in which the hydroxylamine moiety is placed above the plane of one of the carbonyl groups of glyoxal moiety. The I<sub>GH</sub> complex with the binding energy of  $-18.25$  kJ mol<sup>-1</sup> is stabilized by the O–H···O(C) bond, as evidenced by the elongation of the O–H and C=O bonds (see Table S2). The intermolecular distance between the oxygen atom of glyoxal and the hydrogen atom of hydroxylamine has a length of 1.988 Å, and the O–H···O angle is equal to 148.2°. In turn, the II<sub>GH</sub> complex ( $\Delta E = -15.35$  kJ mol<sup>-1</sup>) is stabilized by N–H···O(C) interaction, which leads to elongation of the N–H and C=O bonds (see Table S2). The ab initio studies performed earlier for the glyoxal–methanol [43] and methylglyoxal–methanol complexes [44] indicated that the nonplanar non-hydrogen-bonded structures are the most stable ones. Decomposition of the interaction energy performed for the glyoxal–methanol complex [43] showed that the relative stability of the isomeric glyoxal complexes results from the subtle interplay between all energy components. However, the calculations indicated also that the dispersion energy contributed more to the stabilization of the non-hydrogen-bonded complex than to the hydrogen-bonded one.

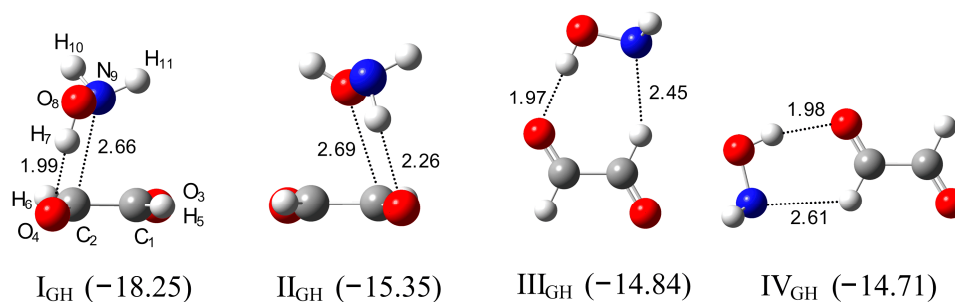


**Figure 3.** The optimized structures of the CHOCHO–NH<sub>2</sub>OH complexes, I<sub>GH</sub>–IV<sub>GH</sub>. The  $\Delta E^{\text{CP}}$  (ZPE)-binding energies in kJ mol<sup>-1</sup> are given in parentheses. The intermolecular distances are given in Å.

The next six complexes are stabilized by two hydrogen bonds and have planar, cyclic structures. Four of them are sustained by the O–H···O(C) bond and additionally by C–H···N (III<sub>GH</sub>, IV<sub>GH</sub>) or C–H···O(N) interaction (V<sub>GH</sub>). Two complexes are stabilized by the N–H···O(C) and C–H···O(N) bonds (VI<sub>GH</sub>, VII<sub>GH</sub>). In III<sub>GH</sub> and IV<sub>GH</sub> complexes, the intermolecular distances between the oxygen atom of Gly and hydrogen atom of HA are equal to 1.970 Å, and 1.980 Å and the O–H···O angle values are equal to 176.9° and 163.3°, respectively. The CH···N bond lengths are predicted as 2.458 Å and 2.609 Å and angles as 151.5° and 118.9°.

**Experimental Spectra.** The infrared spectra of the Gly/Ar(N<sub>2</sub>), HA/Ar(N<sub>2</sub>) and d-HA/Ar(N<sub>2</sub>) matrices agree well with those reported in the literature [48,49,56,59,60]. In the spectra of the matrices doped both with glyoxal and hydroxylamine, a set of new absorptions appeared in the vicinity of Gly and HA or d-HA absorptions that can be assigned to the complexes formed between glyoxal and hydroxylamine. The selected regions of the spectra of Gly/HA/Ar and Gly/HA/N<sub>2</sub> are presented in Figures 4 and 5, respectively. The bands assigned to the glyoxal–hydroxylamine complexes are marked by the arrows. The wavenumbers of all observed complex bands are collected in Table 2 and Table S3 in Supplementary Material. The results obtained in experiments with the deuterated hydroxylamine are presented in Figures S3 and S4 and in Table S4 in Supplementary Material.

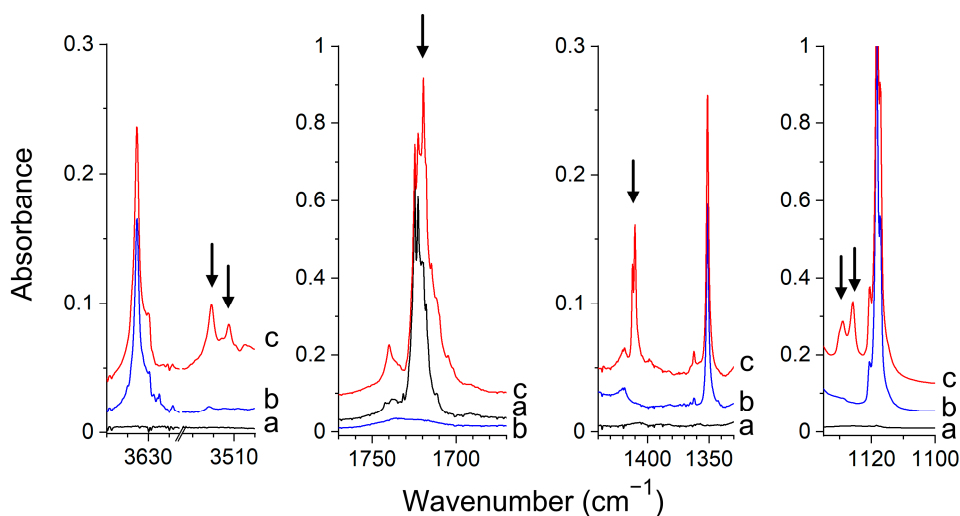


**Figure 4.** The spectra of the CHOCHO/Ar (a), NH<sub>2</sub>OH/Ar (b) and CHOCHO/NH<sub>2</sub>OH/Ar (c) matrices recorded after matrix deposition at 11 K. The bands of the CHOCHO–NH<sub>2</sub>OH complex are indicated by the arrows.

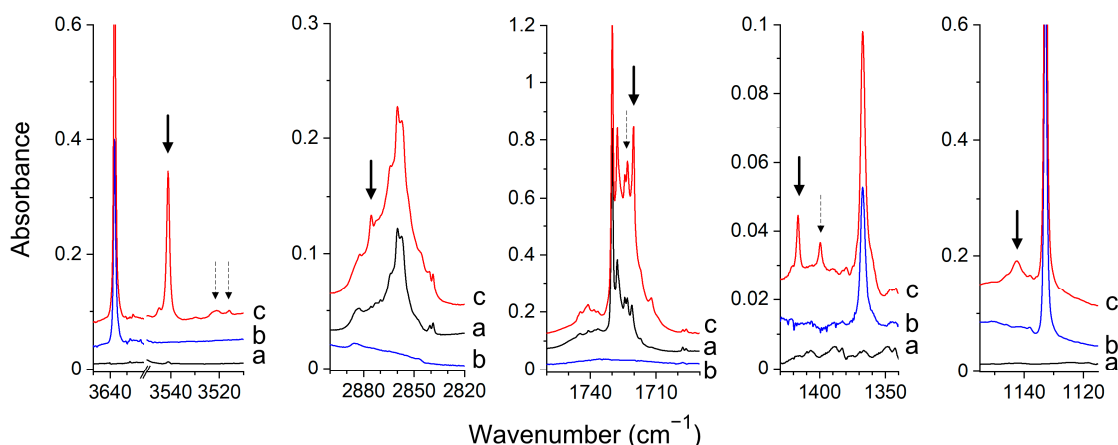


**Figure 5.** The spectra of the CHOCHO/N<sub>2</sub> (a), NH<sub>2</sub>OH/N<sub>2</sub> (b) and CHOCHO/NH<sub>2</sub>OH/N<sub>2</sub> (c) matrices recorded after matrix deposition at 11 K. The bands of CHOCHO–NH<sub>2</sub>OH complexes are indicated by the arrows. Solid and dashed arrows correspond to the III<sub>GH</sub> and I<sub>GH</sub> structures, respectively.

Based on the experimental data and calculated wavenumber shifts, we have assigned the new bands in the spectra of an argon matrix to the nonplanar I<sub>GH</sub> structure. In the nitrogen matrix, both the doubly hydrogen-bonded cyclic structure corresponding to III<sub>GH</sub> and the nonplanar I<sub>GH</sub> complex were found formed, as discussed below. In the spectra of argon matrices, the  $\nu(\text{OH})$  band of the complexed hydroxylamine is distinctly shifted to lower wavenumbers, which suggests the formation of the hydrogen-bonded complex. The observed  $\Delta\nu(\text{OH})$  value,  $-118.8 \text{ cm}^{-1}$ , matches quite well the predicted value of  $-145 \text{ cm}^{-1}$  for the structure I<sub>GH</sub>. The intensity of the  $\nu(\text{OH})$  band is comparable with the intensities of the other strong bands of the complex as predicted for I<sub>GH</sub> by calculations. The observed, large shift ( $+60.9 \text{ cm}^{-1}$ ) of the  $\delta(\text{NOH})$  band of hydroxylamine after complex formation agrees well with the calculated value for I<sub>GH</sub>, equal to  $+61.0 \text{ cm}^{-1}$ . In an experiment with deuterated hydroxylamine, the wavenumbers shifts for the  $\nu(\text{OD})$  and  $\delta(\text{NOD})$  modes are equal to  $-84.1 \text{ cm}^{-1}$  and  $+33.5 \text{ cm}^{-1}$ , respectively. These values agree with the calculated ones equal to  $-106 \text{ cm}^{-1}$  and  $+38 \text{ cm}^{-1}$ . The other experimental wavenumber shifts of the identified complex bands also match well those calculated for the I<sub>GH</sub> structure.

**Table 2.** The comparison of the observed wavenumbers ( $\text{cm}^{-1}$ ) and wavenumber shifts ( $\Delta\nu = \nu_{\text{GH}} - \nu_{\text{M}}$ ) for the CHOCHO-NH<sub>2</sub>OH (GH) complexes present in the Ar and N<sub>2</sub> matrices with the corresponding calculated values for the complexes I<sub>GH</sub>, III<sub>GH</sub> and IV<sub>GH</sub>. In parentheses, the calculated band intensities are given ( $\text{km mol}^{-1}$ ).

Approximate Description	Experimental						Calculated		
	Ar			N <sub>2</sub>			$\Delta\nu$		
	$\nu_{\text{M}}$	$\nu_{\text{GH}}$	$\Delta\nu^1$	$\nu_{\text{M}}$	$\nu_{\text{GH}}^2$	$\Delta\nu^1$	I <sub>GH</sub>	III <sub>GH</sub>	IV <sub>GH</sub>
<b>Hydroxylamine</b>									
$\nu(\text{OH})$	3635.5	3521.0 3512.4	−118.8	3637.6	3541.1 3520.9 3515.8	−96.5 −119.2	−145 (7)	−106 (383)	−103 (356)
$\delta(\text{NOH})$	1351.2	1412.1 1410.2	+60.9	1367.4	1416.6 1399.7	+49.2 +32.3	+61 (63)	+72 (29)	+71 (34)
$\omega(\text{NH}_2)$	1118.3	1129.0 1125.8	+9.1	1133.0	1142.6	+9.6	+14 (11)	+24 (112)	+22 (122)
$\nu(\text{NO})$	895.6			895.3	898.8	+3.5	+14 (3)	+9 (8)	+6 (8)
<b>Glyoxal</b>									
$\nu(\text{CH})$	2860.1 2854.9	2857.6	−0.4	2857.1	2875.6	+18.5	−9 (60) +12 (39)	+15 (53) +20 (1)	+1 (52) +51 (8)
$\nu(\text{C=O})$	1724.5	1719.0	−5.5	1730.1	1720.2 1723.1	−9.9 −7.0	−4 (122) +4 (23)	−11 (126) −6 (20)	−13 (89) −6 (33)
$\gamma(\text{CH})$	812.1 807.8			807.4	820.8	+13.4	+37 (0)	+23 (8)	+16 (2)

<sup>1</sup> In the case when the splitting of the band was observed, the average of the two wavenumbers at which the two peaks appeared was taken into account to calculate  $\Delta\nu$  value. <sup>2</sup> The wavenumbers in italic are due to complex of different structure (see text).

The noticeable difference between the spectra of the complex trapped in solid argon and the one trapped in solid nitrogen is strong  $\nu(\text{OH})$  absorption in nitrogen spectra, which is much more intense than the other bands of the complex (see Figure 5). This is not the case for the argon spectra. For example, the estimated experimental intensity ratios  $(I_{\nu(\text{OH})}/I_{\delta(\text{NOH})})_{\text{exp}}$ ,  $(I_{\nu(\text{OH})}/I_{\omega(\text{NH}_2)})_{\text{exp}}$  are equal to ca. 0.8, 0.4 for the complex identified in the argon matrix, and they increase to ca. 12, 4, respectively, for the complex trapped in the nitrogen matrix. Such experimental intensity ratios match well the calculated ones for the  $\nu(\text{OH})$  absorptions of the nonplanar I<sub>GH</sub> and cyclic planar III<sub>GH</sub> (IV<sub>GH</sub>) complexes. The calculated ratios  $(I_{\nu(\text{OH})}/I_{\delta(\text{NOH})})_{\text{calc}}$ ,  $(I_{\nu(\text{OH})}/I_{\omega(\text{NH}_2)})_{\text{calc}}$  are equal to ca. 1.2, 0.7 for I<sub>GH</sub> and ca. 13, 3.5 for III<sub>GH</sub> (for IV<sub>GH</sub> similar intensity ratios are obtained as for III<sub>GH</sub>). The observed  $\nu(\text{OH})$  shift for the complex trapped in nitrogen ( $-96.5 \text{ cm}^{-1}$ ) is slightly less than that for the complex in argon ( $-118.8 \text{ cm}^{-1}$ ), which is in accord with the shifts predicted for III<sub>GH</sub>, IV<sub>GH</sub> and I<sub>GH</sub> ( $-106$ ,  $-103$ ,  $-145 \text{ cm}^{-1}$ , respectively). The experimental shift of the  $\nu(\text{CH})$  vibration ( $+18.5 \text{ cm}^{-1}$ ) suggests that the III<sub>GH</sub> complex and not the IV<sub>GH</sub> one is created in the nitrogen matrix. The  $+18.5 \text{ cm}^{-1}$  shift matches better with the  $+15 \text{ cm}^{-1}$  value predicted for the III<sub>GH</sub> structure than with the  $+1$  value calculated for IV<sub>GH</sub>. The wavenumber shifts of the other identified vibrations are also in accord with the calculated ones for the III<sub>GH</sub> structure (see Table 2 and Table S3). The significant red-shift of  $\nu(\text{OH})$  of glyoxal accompanied by a noticeable blue shift of  $\nu(\text{CH})$  after complex formation indicates that the III<sub>GH</sub> complex isolated in solid nitrogen is stabilized both by the O–H⋯O(C) hydrogen bond and by blue-shifting C–H⋯N hydrogen bond. The blue shift of the  $\nu(\text{X-H})$  stretching wavenumber of the proton donor after complex formation is characteristic of the blue-shifting hydrogen bonding, also called the improper hydrogen bond. These bonds, formed mainly by the CH proton donors, have been a subject of intense theoretical [61–66] and experimental studies [65,66].

All the bands identified for the  $I_{GH}$  complex in the spectra of the argon matrices, as well as all the bands assigned to the  $III_{GH}$  complex in the spectra of solid nitrogen, exhibited the same intensity ratios in all performed experiments as expected for the bands due to the same species. However, in the spectra of the CHOCHO/NH<sub>2</sub>OH/N<sub>2</sub> matrices, in addition to the bands attributed to  $III_{GH}$  (marked by solid arrows in Figure 5), three additional bands appeared (marked by dashed arrows in Figure 5) whose relative intensities were the same with respect to each other in the performed experiments however differed with respect to the absorptions assigned to  $III_{GH}$ . The bands appeared as a very weak doublet at 3520.9, 3515.8 cm<sup>-1</sup>, and as single absorptions at 1723.1, 1399.7 cm<sup>-1</sup> in the region of the  $\nu(\text{OH})$ ,  $\nu(\text{C}=\text{O})$  and  $\delta(\text{NOH})$  vibrations, respectively. The shifts of these bands with respect to the corresponding absorptions of the parent molecules ( $\Delta\nu(\text{OH}) = -116.7, -121.8 \text{ cm}^{-1}$ ,  $\Delta\nu(\text{C}=\text{O}) = -7.0 \text{ cm}^{-1}$  and  $\delta(\text{NOH}) = +32.4 \text{ cm}^{-1}$ ) and their relative intensities indicate that they are due to the CHOCHO–NH<sub>2</sub>OH complex of the  $I_{GH}$  structure. The concentration ratio of the complexes  $III_{GH}/I_{GH}$  was estimated on the basis of the  $\nu(\text{OH})$  and  $\delta(\text{NOH})$  absorptions ( $(I_{\text{exp}}(III_{GH})/I_{\text{exp}}(I_{GH})) \times (I_{\text{calc}}(I_{GH})/I_{\text{calc}}(III_{GH}))$ ) and was found to be ca. 3:2. The change of the conditions of matrix deposition (concentration, depositions temperature) slightly affected the mutual concentration of the two structures.

Mucha and Mielke studied the glyoxal complexes with water and hydrogen peroxide in the argon matrices [42,45]. Gly–H<sub>2</sub>O and Gly–H<sub>2</sub>O<sub>2</sub> complexes isolated in solid argon have planar, cyclic structures analogous to the  $III_{GH}$  one. The observed shifts of the  $\nu(\text{C}-\text{H})$ ,  $\nu(\text{C}=\text{O})$  wavenumbers of glyoxal are equal to +2.5, –0.6 cm<sup>-1</sup>, respectively, for the Gly–H<sub>2</sub>O complex; and to +28.9, +3.3 cm<sup>-1</sup> ( $\nu_s(\text{CH})$ ,  $\nu_{\text{as}}(\text{CH})$ ), –5.0 cm<sup>-1</sup> ( $\nu(\text{C}=\text{O})$ ) for the Gly–H<sub>2</sub>O<sub>2</sub> one as compared to +18.5, –9.9 cm<sup>-1</sup>, respectively, for Gly–NH<sub>2</sub>OH,  $III_{GH}$ . The observed perturbations of glyoxal vibrations in the above complexes indicate that the glyoxal complex with hydroxylamine is much stronger than that with water, and its strength is comparable to the complex with hydrogen peroxide. This is in accord with the calculated energy values for the above complexes (ca. –11, –17 and –18 kJ mol<sup>-1</sup> for Gly–H<sub>2</sub>O, Gly–NH<sub>2</sub>OH and Gly–H<sub>2</sub>O<sub>2</sub>, respectively) [42,45].

### 2.3. Methylglyoxal–Hydroxylamine Complexes

*Ab Initio Calculations.* Methylglyoxal, like glyoxal, in the standard conditions exists only as of the *trans* isomer [67], so only this conformer is considered in our study. The predicted structures of the complexes formed between methylglyoxal and hydroxylamine are presented in Figure 6 (eight most stable structures) and in Figure S5 in Supplementary Material (all fifteen structures). The geometrical parameters are listed in Table S5.

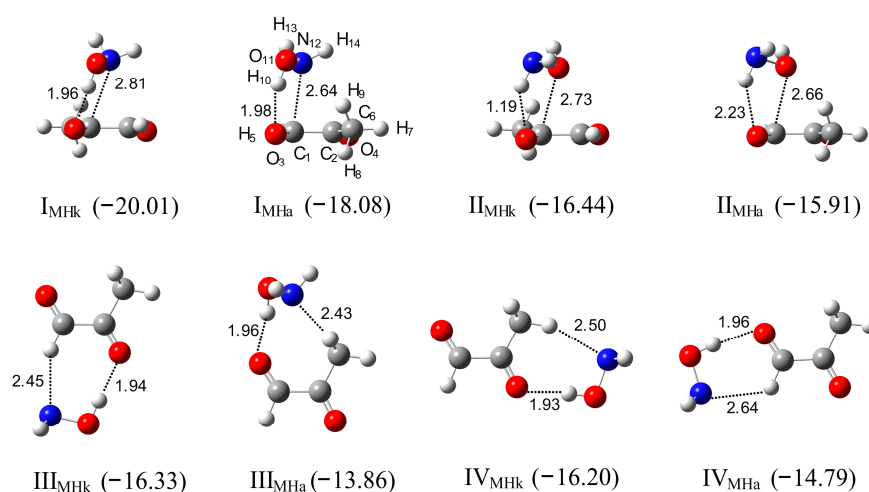


**Figure 6.** The optimized structures of the CH<sub>3</sub>COCHO–NH<sub>2</sub>OH complexes, I<sub>MHk</sub>–IV<sub>MHk</sub> and I<sub>MHa</sub>–IV<sub>MHa</sub>. The intermolecular distances are given in Å. The  $\Delta E^{\text{CP}}(\text{ZPE})$ -binding energies in kJ mol<sup>-1</sup> are given in parentheses.

The structures of the MGly–HA complexes are analogous to the structures predicted for the Gly–HA ones. The two most stable structures,  $I_{\text{MHK}}$  and  $I_{\text{MHa}}$ , with the binding energies of about  $-20$  and  $-18$   $\text{kJ mol}^{-1}$ , are nonplanar. In  $I_{\text{MHK}}$ , the hydroxylamine moiety is placed above the acetyl group and in  $I_{\text{MHa}}$  above the aldehyde group of methylglyoxal. These complexes are stabilized by the  $\text{O–H} \cdots \text{O}(\text{C})$  interaction between the oxygen atom of the aldehyde or acetyl group of methylglyoxal and the OH group of hydroxylamine. The formation of the hydrogen bond is manifested by the elongation of the  $\text{O–H}$  bond of hydroxylamine from  $0.959$   $\text{\AA}$  to  $0.968$   $\text{\AA}$ . The intermolecular  $\text{H} \cdots \text{O}$  distances and  $\text{O–H} \cdots \text{O}(\text{C})$  angles are equal to  $1.956$   $\text{\AA}$ ,  $151.5^\circ$  for  $I_{\text{MHK}}$  and  $1.980$   $\text{\AA}$ ,  $148.6^\circ$  for  $I_{\text{MHa}}$ . The nonplanar structures  $II_{\text{MHK}}$  and  $II_{\text{MHa}}$  are stabilized by  $\text{N–H} \cdots \text{O}(\text{C})$  interaction. The other predicted complexes have cyclic forms stabilized by two hydrogen bonds. Structures  $III_{\text{MHK}}$ ,  $III_{\text{MHa}}$ ,  $IV_{\text{MHK}}$ ,  $IV_{\text{MHa}}$ ,  $V_{\text{MHK}}$ ,  $V_{\text{MHa}}$ ,  $VI_{\text{MHK}}$  and  $VI_{\text{MHa}}$  are stabilized by the  $\text{O–H} \cdots \text{O}(\text{C})$  and, additionally, by  $(\text{O})\text{C–H} \cdots \text{N}$  or  $\text{H}_2\text{C–H} \cdots \text{N}$  interactions and the complexes  $VII_{\text{MHK}}$ ,  $VIII_{\text{MHK}}$ ,  $VIII_{\text{MHa}}$  by the  $\text{N–H} \cdots \text{O}(\text{C})$  hydrogen bond and by  $(\text{O})\text{C–H} \cdots \text{O}$  or  $\text{H}_2\text{C–H} \cdots \text{N}$  interaction.

**Experimental Spectra.** In Figure 7 and Figure S6 (Supplementary Material), the infrared spectra of doubly doped MGly/HA/Ar, MGly/d-HA/Ar matrices are compared with the singly doped MGly/Ar, HA/Ar, d-HA/Ar matrices. In Figure 8, the result of the experiment carried in solid nitrogen is presented. The infrared spectra of MGly agree well with those reported earlier [42,60,68]. The new bands that appeared in the spectra of doubly doped matrices are marked by the arrows and are assigned to the MGly–HA,  $I_{\text{MHa}}$  complex.

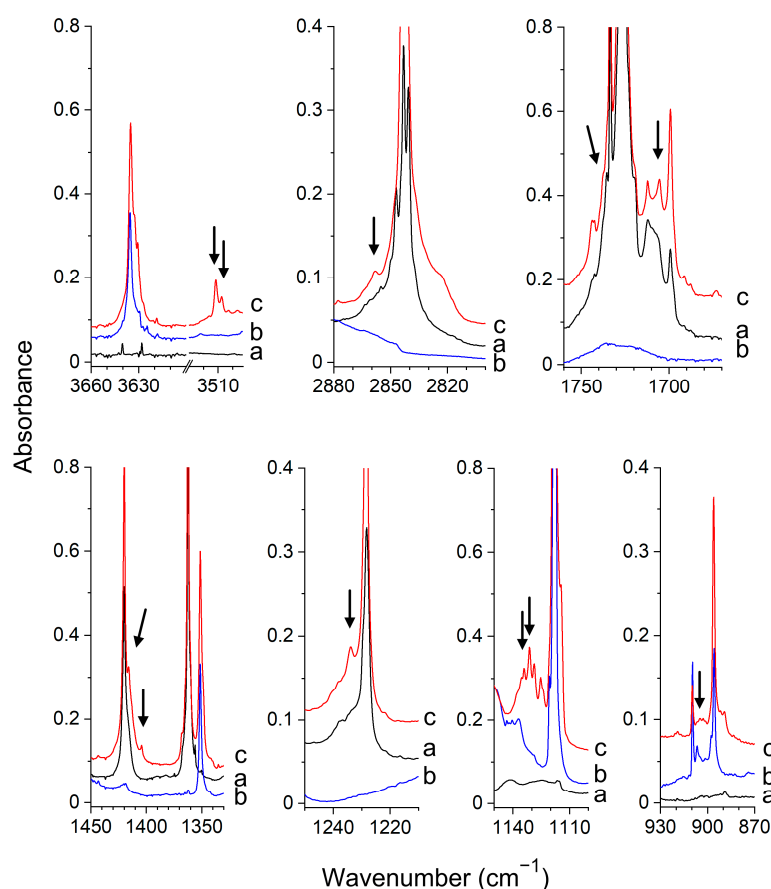


**Figure 7.** The spectra of the  $\text{CH}_3\text{COCHO}/\text{Ar}$  (a),  $\text{NH}_2\text{OH}/\text{Ar}$  (b) and  $\text{CH}_3\text{COCHO}/\text{NH}_2\text{OH}/\text{Ar}$  (c) matrices recorded after matrix deposition at 11 K. The bands of the  $\text{CH}_3\text{COCHO–NH}_2\text{OH}$  complex are indicated by the arrows.

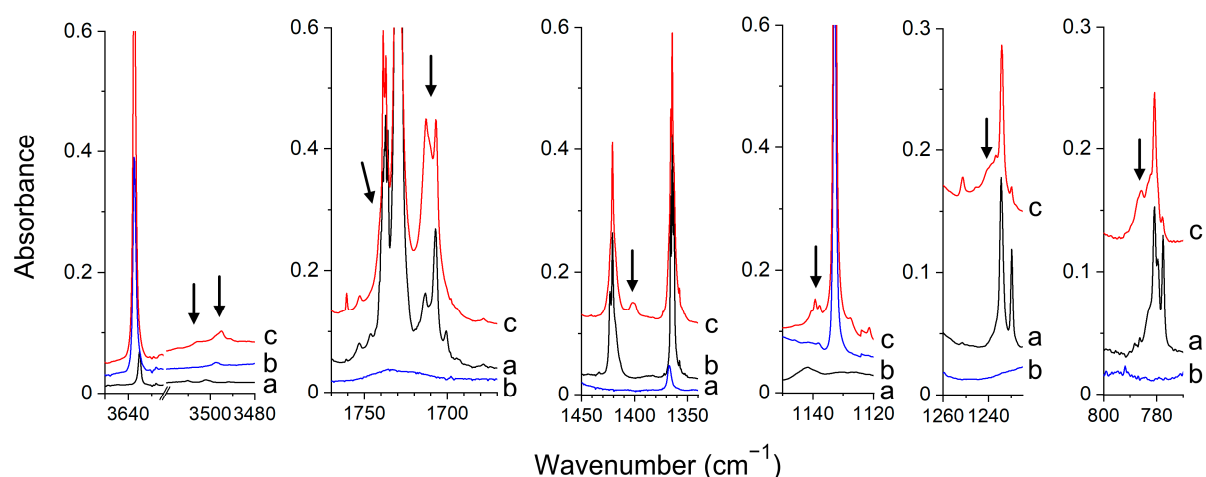


**Figure 8.** The spectra of the  $\text{CH}_3\text{COCHO}/\text{N}_2$  (a),  $\text{NH}_2\text{OH}/\text{N}_2$  (b) and  $\text{CH}_3\text{COCHO}/\text{NH}_2\text{OH}/\text{N}_2$  (c) matrices recorded after matrix deposition at 11 K. The bands of  $\text{CH}_3\text{COCHO}-\text{NH}_2\text{OH}$  complex are indicated by the arrows.

Analysis of the spectra shows that in doubly doped argon and nitrogen matrices, the same type of hydrogen-bonded complex is formed. The comparison of our experimental data with the theoretical ones (see Table 3, Tables S6 and S7 in Supplementary Material) indicates that the isolated complex has a structure  $I_{\text{MHa}}$ , as discussed below. The new band due to the  $\nu(\text{OH})$  vibration of the  $\text{MGly}-\text{HA}$  complex is shifted 125.8, 137.1  $\text{cm}^{-1}$  towards lower wavenumbers in the spectra of argon and nitrogen matrices, respectively. The red-shift of the  $\nu(\text{OH})$  is accompanied by the blue shift of  $\delta(\text{NOH})$ . The latter vibration is coupled in the complex with the perturbed  $\delta(\text{CH}_3)$  vibration. The coupling is supported by the  $\text{CH}_3\text{COHCO}-\text{ND}_2\text{OD}$  spectra in which neither of the two bands is observed (when  $\delta(\text{NOD})$  is shifted to lower wavenumbers and not coupled with  $\delta(\text{CH}_3)$ , the latter band may be too weak to be observed). Two bands that are assigned to the coupled  $\delta(\text{NOH}) + \delta(\text{CH}_3)$  vibrations appear at 1404.1, 1416.1  $\text{cm}^{-1}$  in the spectra of an argon matrix. In the nitrogen matrix, only one new band was identified in the region of the  $\delta(\text{NOH})$ , which is shifted +34.1  $\text{cm}^{-1}$  from the corresponding monomer band. The above facts indicate that the OH group of hydroxylamine interacts with the methylglyoxal molecule forming the  $\text{O}-\text{H} \cdots \text{O}(\text{C})$  hydrogen bond and allow to exclude all structures in which this bond is not formed ( $II_{\text{MHa}}$ ,  $II_{\text{MHk}}$ ,  $VII_{\text{MHk}}$ ,  $VIII_{\text{MHa}}$ ,  $VIII_{\text{MHk}}$ ). The intensity of the  $\nu(\text{OH})$  band is comparable (or slightly larger) to the intensities of the other most intense bands ( $\delta(\text{NOH})$ ,  $\omega(\text{NH}_2)$ ,  $\nu(\text{C}=\text{O})$ ) of  $\text{MGly}-\text{HA}$  complex in the spectra of Ar and  $\text{N}_2$  matrices as can be seen in Figures 7 and 8. This is in accord with the predicted intensities for the  $I_{\text{MHa}}$ ,  $I_{\text{MHk}}$  complexes and allows us to eliminate the cyclic structures  $III_{\text{MHa}}$ ,  $III_{\text{MHk}}$ ,  $IV_{\text{MHa}}$ ,  $IV_{\text{MHk}}$  for, which the  $\nu(\text{OH})$  is predicted to be ca. 3.5–5 times more intense than the second most intense band of the complex (see Table 3 and Table S6). The other spectral features of the recorded spectra point to the presence of  $I_{\text{MHa}}$  in the matrix. The observed shifts of the  $\nu_{\text{ket}}(\text{C}=\text{O})$  and  $\nu_{\text{ald}}(\text{C}=\text{O})$  bands of  $\text{MGly}$  after complexation are equal to +4.2 and  $-21.0$  in Ar (+3.9 and  $-18.2$   $\text{cm}^{-1}$  in  $\text{N}_2$  matrix, respectively), which suggests that in the complex the OH group of HA is interacting with the oxygen atom of the aldehyde group and not with acetyl one. The corresponding calculated shifts of the  $\nu_{\text{ket}}(\text{C}=\text{O})$  and  $\nu_{\text{ald}}(\text{C}=\text{O})$  bands are equal to +4,  $-10$   $\text{cm}^{-1}$  for  $I_{\text{MHa}}$  and  $-5$ , +6  $\text{cm}^{-1}$  for  $I_{\text{MHk}}$ , respectively. The observed shift of the CH stretch of the aldehyde group (+16.3  $\text{cm}^{-1}$  in Ar) confirms that  $I_{\text{MHa}}$  is formed and not  $I_{\text{MHk}}$ . The calculated  $\Delta\nu$  shifts for CH stretch vibration are equal to  $-1$ , +24  $\text{cm}^{-1}$  for  $I_{\text{MHk}}$ ,  $I_{\text{MHa}}$ , respectively. The observed shifts of all other bands identified for the complex present in the Ar,  $\text{N}_2$  matrices also match well the predicted ones for the  $I_{\text{MHa}}$  complex.

**Table 3.** The comparison of the observed wavenumbers ( $\text{cm}^{-1}$ ) and wavenumber shifts ( $\Delta\nu = \nu_{\text{MH}} - \nu_{\text{M}}$ ) for the  $\text{CH}_3\text{COCHO-NH}_2\text{OH}$  (MH) complexes present in the Ar and  $\text{N}_2$  matrices with the corresponding calculated values for the complexes  $\text{I}_{\text{MHK}}$  and  $\text{I}_{\text{MHa}}$ . In parentheses, the calculated band intensities are given ( $\text{km mol}^{-1}$ ).

Approximate Description	Experimental						Calculated	
	Ar			$\text{N}_2$			$\Delta\nu$	
	$\nu_{\text{M}}$	$\nu_{\text{MH}}$	$\Delta\nu^1$	$\nu_{\text{M}}$	$\nu_{\text{MH}}$	$\Delta\nu^1$	$\text{I}_{\text{MHK}}$	$\text{I}_{\text{MHa}}$
<b>Hydroxylamine</b>								
$\nu(\text{OH})$	3635.5	3511.7 3507.6	−125.8	3637.6	3505.7 3495.2	−137.1	−148 (138)	−156 (73)
$\delta(\text{NOH})^2$	1351.2	1404.1	+52.9	1367.4	1402.7 1400.3	+34.1	+64 (58)	+62 (51)
$\omega(\text{NH}_2)$	1118.3	1134.1 1131.2	+14.4	1133.0	1139.3 1140.6	+7.0	+17 (117)	+11 (109)
$\nu(\text{NO})$	895.6	904.8 902.9	+8.3	895.3			+9 (5)	+13 (6)
<b>Methylglyoxal</b>								
$\nu(\text{CH})$	2843.1 2840.7	2858.2	+16.3	2844.7 2840.2 2835.9			−1 (60)	+24 (51)
$\nu_{\text{ket}}(\text{C=O})$	1733.5	1737.7	+4.2	1739.0 1737.2 1735.9	1741.3	+3.9	−5 (132)	+4 (61)
$\nu_{\text{ald}}(\text{C=O})$	1726.4	1705.4	−21.0	1730.1 1727.9	1710.8	−18.2	+6 (27)	−10 (97)
$\delta(\text{CH}_3)^2$	1420.0	1416.1	−3.9	1423.2 1420.8			0 (8) +3 (24) −3 (36)	+5 (6) +3 (25) −2 (31)
$\nu_{\text{as}}(\text{C-C})$	1228.3	1233.7	+5.4	1234.5 1229.9	1240.5 1237.1	+6.6	+5 (14)	+5 (15)
$\nu_{\text{s}}(\text{C-C})$	777.1	784.7	+7.6	780.9 779.5 777.6	785.8 782.3	+4.8	+6 (15)	+6 (15)

<sup>1</sup> In the case when the splitting of the band was observed, the average of the two wavenumbers at which the two peaks appear was taken into account to calculate  $\Delta\nu$  value. <sup>2</sup> The 1416.1, 1404.1  $\text{cm}^{-1}$  bands observed in the spectra of the complex in Ar matrix are assigned to the coupled  $\delta(\text{NOH})+\delta(\text{CH}_3)$  vibrations.

We have found no sign of formation of any cyclic MGly–HA complex. In contrast, the interaction of methylglyoxal with water and methanol forms exclusively the cyclic planar complexes stabilized by the  $\text{O-H}\cdots\text{O}(\text{C})$  and  $\text{C-H}\cdots\text{O}$  hydrogen bonds between the OH group of  $\text{H}_2\text{O}$  or  $\text{CH}_3\text{OH}$  and the acetyl or aldehyde oxygen atom of  $\text{CH}_3\text{COCHO}$  [42,44]. The presence of the less stable complex  $\text{I}_{\text{MHa}}$  than the more stable  $\text{I}_{\text{MHK}}$  is probably due to the steric effects between the hydroxylamine moiety and methyl group of methylglyoxal.

#### 2.4. AIM Analysis

In Figures S7 and S8 (Supporting Information), the location of the bond critical points (BCP) and ring critical points (RCP) in all optimized structures of the formaldehyde–hydroxylamine and glyoxal–hydroxylamine complexes are presented. The AIM parameters of intermolecular BCPs are collected in Table 4. The general classification of the interaction type can be performed using topological parameters [69,70]. The investigation of Laplacian of electron density ( $\nabla^2\rho_{\text{b}}$ ) indicates if there is a local concentration ( $\nabla^2\rho_{\text{b}} < 0$ ) or a local depletion ( $\nabla^2\rho_{\text{b}} > 0$ ) of charge. Low  $\rho_{\text{b}}$  and  $\nabla^2\rho_{\text{b}}$  values and total electron energy  $H \approx 0$  indicate that the complexes are stabilized by weak hydrogen bonds or van der Waals

interaction. The criteria for the presence of hydrogen bond limit the lower values of the electron density,  $\rho_b$ , and the Laplacian of the electron density,  $\nabla^2\rho_b$ , to 0.002, 0.024 a.u., respectively, and the corresponding upper values to 0.034, 0.139 a.u.

**Table 4.** AIM properties of selected critical points computed at the MP2/6-311++G(2d,2p) level. All data reported in atomic units.

Complex	BCP	$\rho_b$	$\nabla^2\rho_b$	Complex	BCP	$\rho_b$	$\nabla^2\rho_b$
<b>Formaldehyde–Hydroxylamine Complexes</b>				<b>Glyoxal–Hydroxylamine Complexes</b>			
I <sub>FH</sub>	O4-H5 <sup>a</sup>	0.0256	0.0855	I <sub>GH</sub>	C2-N9	0.0203	0.0626
	H2-N7 <sup>c</sup>	0.0090	0.0268		O4-H7 <sup>a</sup>	0.0213	0.0800
II <sub>FH</sub>	O4-H5 <sup>a</sup>	0.0207	0.0791	II <sub>GH</sub>	C1-O8	0.0158	0.0582
	C1-N7	0.0160	0.0514		O3-H10 <sup>b</sup>	0.0129	0.0472
III <sub>FH</sub>	O4-H5 <sup>a</sup>	0.0226	0.0798	III <sub>GH</sub>	O4-H7 <sup>a</sup> H5-N9 <sup>d</sup>	0.0225 0.0122	0.0772 0.0342
IV <sub>FH</sub>	O4-H8 <sup>b</sup>	0.0164	0.0560	IV <sub>GH</sub>	O4-H7 <sup>a</sup> H6-N9 <sup>d</sup>	0.0227 0.0097	0.0782 0.0290
	H2-O6 <sup>c</sup>	0.0099	0.0337				
V <sub>FH</sub>	C1-O6	0.0131	0.0478	V <sub>GH</sub>	O4-H7 <sup>a</sup> H5-O8 <sup>c</sup>	0.0194 0.0107	0.0687 0.0404
	O4-H8 <sup>b</sup>	0.0136	0.0513				
				VI <sub>GH</sub>	O4-H10 <sup>b</sup> H5-O8 <sup>c</sup>	0.0143 0.0126	0.0494 0.0414
				VII <sub>GH</sub>	H6-O8 <sup>c</sup> O4-H10 <sup>b</sup>	0.0108 0.0144	0.0370 0.0499
				VIII <sub>GH</sub>	O4-H7 <sup>a</sup>	0.0186	0.0690

<sup>a</sup> OH...O path, <sup>b</sup> NH...O path, <sup>c</sup> CH...O path, <sup>d</sup> CH...N path.

The inspection of the results presented in Figure S7 and Table 4 shows that the HCHO–NH<sub>2</sub>OH complexes are stabilized by OH...O, NH...O, CH...O and CH...N interactions. In two complexes, the N...C or O...C interaction occurs (II<sub>FH</sub>, V<sub>FH</sub>, respectively). For the OH...O and NH...O interactions, the  $\rho_b$  values are in the range  $0.0136 < \rho_b < 0.0256$  a.u., and positive Laplacian  $\nabla^2\rho_b$ , is in the range  $0.0513 < \nabla^2\rho_b < 0.0855$  a.u., such values are characteristic of hydrogen bonds. The structures I<sub>FH</sub>, II<sub>FH</sub>, IV<sub>FH</sub> and V<sub>FH</sub>, are characterized by two intermolecular bond critical points, BCP, and one ring critical point, RCP. The structure III<sub>FH</sub> involves only one BCP on the bond path corresponding to the interaction between the oxygen atom of formaldehyde and the hydrogen atom of the hydroxyl group of the hydroxylamine molecule. For the bonding in which the hydrogen atom of the CH group is involved (structures I<sub>FH</sub> and IV<sub>FH</sub>), the electron densities values fall within the range:  $0.009 < \rho_b < 0.01$  a.u., and the Laplacian in the range:  $0.0268 < \nabla^2\rho_b < 0.0337$  a.u. These parameters indicate that a very weak hydrogen bond is responsible for the formation of CH...N and CH...O interactions. Data in Table 4 show that the highest values of the discussed parameters occurred for the complex I<sub>FH</sub>, which is the most stable one according to calculations.

The topological analysis indicates that the structures of the CHOCHO–NH<sub>2</sub>OH complex are maintained by similar types of interactions as the configurations of the hydroxylamine complex with formaldehyde. In the glyoxal complexes, like in the formaldehyde ones, one BCP point corresponds to the OH...O or NH...O interaction and the second one to the CH...N or CH...O interaction which involves the hydrogen atom one of the two CH groups. In the nonplanar glyoxal complexes, one BCP corresponds to the OH...O or NH...O hydrogen bonding and the second one to the N...C or O...C interaction (I<sub>GH</sub>, II<sub>GH</sub>). The AIM parameters of BCPs along OH...O in the glyoxal complexes (I<sub>GH</sub>, III<sub>GH</sub>, IV<sub>GH</sub>, V<sub>GH</sub>, VIII<sub>GH</sub>) have very close values:  $\rho_b \approx 0.02$  a.u.,  $\nabla^2\rho_b \approx 0.07$  a.u. as well as the:  $\rho_b \approx 0.013$  a.u.,  $\nabla^2\rho_b \approx 0.05$  a.u. values calculated for the NH...O bond paths (II<sub>GH</sub>, VI<sub>GH</sub>, VII<sub>GH</sub>). It is interesting to notice that the structures I and II of the CHOCHO–NH<sub>2</sub>OH

complexes, like the structures II and V of the HCHO–NH<sub>2</sub>OH system, involve one BCP on the bond path corresponding to the interaction between the nitrogen or oxygen atoms of hydroxylamine and the carbon atom of the glyoxal or formaldehyde molecule. The BCPs parameters for the bond paths involving CH···O or CH···N interactions in the CHOCHO–NH<sub>2</sub>OH complex have slightly larger values ( $\rho_b \approx 0.01$  a.u. and  $\nabla^2\rho \approx 0.04$  a.u.) than those characterizing analogous interactions in the HCHO–NH<sub>2</sub>OH complex.

The classification of the OH···O, NH···O interactions in all configurations of the HCHO–NH<sub>2</sub>OH and CHOCHO–NH<sub>2</sub>OH complexes as a hydrogen bonding interaction is strongly confirmed both by experimental and theoretical data and is free from doubt. The electron density and Laplacian values in the BCPs on the O···H and N···H bond paths are within the range characteristic for the hydrogen bonding. The large perturbations of the OH or NH stretching vibrations accompanied by perturbations of the carbonyl group vibrations, as demonstrated in the recorded infrared spectra of the hydroxylamine complexes, provide strong evidence of the formation of the O–H···O or N–H···O bonds. The other important interactions stabilizing the studied complexes are the ones in which the hydrogen atoms of the CH group of the carbonyl molecule are involved.

### 2.5. Hydrogen Bonding in the Carbonyl-Hydroxylamine Complexes

The results of our experimental and theoretical studies show that all studied carbonyl compounds (formaldehyde, glyoxal and methylglyoxal) form the hydrogen-bonded complexes with hydroxylamine in the argon and nitrogen matrices. The structures attributed to the complexes are gathered in Figures S9 and S10 in Supporting Information. FA was found to form the cyclic planar structure, I<sub>FH</sub>, and MGly the nonplanar one, I<sub>MHa</sub>, in both argon and nitrogen matrices. In turn, Gly forms the nonplanar complex, I<sub>GH</sub>, in the argon matrix, whereas in the nitrogen matrix, both the cyclic planar, III<sub>GH</sub>, structure and the nonplanar one are created.

The topological analysis indicated the following types of hydrogen bonding in the hydroxylamine complexes with formaldehyde and glyoxal, namely: OH···O, NH···O and CH···O, CH···N. In addition, in two FA complexes and two Gly ones, the analysis indicated the N···C and O···C interactions (II<sub>FH</sub>, I<sub>GH</sub> and V<sub>FH</sub>, II<sub>GH</sub>, respectively). The most stable HCHO–NH<sub>2</sub>OH complex, I<sub>FH</sub>, observed in the argon and nitrogen matrices, is stabilized by two hydrogen bonds, OH···O and CH···N. In turn, the most stable CHOCHO–NH<sub>2</sub>OH complex, I<sub>GH</sub>, is stabilized by the OH···O hydrogen bond and N···C interaction; this complex is formed both in argon and nitrogen matrix. In the nitrogen matrix, the less stable, cyclic complex, III<sub>GH</sub>, stabilized by two hydrogen bonds, OH···O and CH···N is also created. Comparison of the predicted structural parameters for the isolated complexes shows that in the cyclic planar complexes, I<sub>FH</sub>, III<sub>GH</sub>, the OH···O(C) intermolecular distance is slightly shorter (0.02–0.06 Å) than in the nonplanar structures, I<sub>GH</sub>, I<sub>MHa</sub>. The formation of the cyclic structures is accompanied by a strong increase of  $\nu(\text{OH})$  intensity in contrast with the nonplanar ones.

In Table 5, the wavenumber shifts of the hydroxylamine vibrations in the complexes with various proton acceptors are compared. It can be observed that in the complexes with formaldehyde, glyoxal and methylglyoxal, the perturbation of hydroxylamine vibrations is quite similar and shows small sensitivity to the carbonyl molecule and to the complex structure. The shifts for carbonyl complexes are comparable with the data reported for the NH<sub>2</sub>OH–H<sub>2</sub>O complex [49] and are much smaller (two/three times) than the values reported for the hydroxylamine complexes with NH<sub>3</sub> [50] and for the hydroxylamine dimer (NH<sub>2</sub>OH)<sub>2</sub> [48] in accord with much stronger interaction in the latter complexes. The smallest perturbation of hydroxylamine vibrations is observed for the NH<sub>2</sub>OH–CO complex identified in the argon matrix, which is much weaker than the complexes of hydroxylamine with formaldehyde and  $\alpha$ -dicarbonyls [51].

**Table 5.** The comparison of wavenumber shifts ( $\text{cm}^{-1}$ ) of the vibrational bands of the hydroxylamine moiety in the complexes with formaldehyde, glyoxal, methylglyoxal, hydroxylamine, carbon monoxide and ammonia observed in argon and nitrogen matrices.

Approximate Description	HCHO		CHOCHO		CH <sub>3</sub> COCHO		NH <sub>2</sub> OH <sup>1</sup>		CO <sup>2</sup>	H <sub>2</sub> O <sup>3</sup>		NH <sub>3</sub> <sup>4</sup>	
	Ar (p) <sup>5</sup>	N <sub>2</sub> (p) <sup>5</sup>	Ar (n) <sup>5</sup>	N <sub>2</sub> (p,n) <sup>5</sup>	Ar (n) <sup>5</sup>	N <sub>2</sub> (n) <sup>5</sup>	Ar	N <sub>2</sub>	Ar	Ar	N <sub>2</sub>	Ar	N <sub>2</sub>
$\nu(\text{OH})$	−115	−125	−119	−97 (p) −119 (n)	−126	−137	−294 −345	−289 −333	−39	−93	−139	−297	−345
$\delta(\text{NOH})$	+70	+60	+61	+49 (p) +34 (n)	+53	+34	+119	+105		+10	+54	+121	+108
$\omega(\text{NH}_2)$ $\omega(\text{NH}_2)$	+20	+24	+9	+10 (p)	+14	+7	+34	+31	+4	+19	+18	+12	+13
$\nu(\text{NO})$		+4	+5	+4 (p)	+8		+14	+9		+12	+19	+10	+8
$\tau(\text{OH})$	+162	+173					+362 +32	+340 +28				+422	+350

<sup>1</sup> Data taken from ref [48]. <sup>2</sup> Data taken from ref [51]. <sup>3</sup> Data taken from ref [49]. <sup>4</sup> Data taken from ref [50]. <sup>5</sup> The wavenumbers shifts of the bands identified for the cyclic, planar (p) and nonplanar complexes (n).

Over the many past decades, there have been many attempts to decode from vibrational spectra the information on the electronic structure of a molecule and about the strength of its bonds. Such information can now be obtained from the local vibrational mode analysis that was originally introduced by Konkoli and Cremer and is becoming increasingly popular [71]. The method was successfully applied to various systems, among them to a number of hydrogen-bonded systems, mainly to homo-aggregates [71–74]. It would be very interesting to apply the local vibrational mode analysis to study the heterodimers between hydroxylamine  $\alpha$ -dicarbonyls in order to get a deeper insight into the bonding of these systems, and such study is planned to be performed in the future.

### 3. Materials and Methods

Formaldehyde, HCHO (FA), was prepared by heating paraformaldehyde (95%, Sigma-Aldrich) up to 65–75 °C directly in the deposition line. Glyoxal, CHOCHO (Gly), was prepared by heating the solid trimer dihydrate (98%, Sigma-Aldrich: St. Louis, MO, USA) topped with phosphorus pentoxide (P<sub>4</sub>O<sub>10</sub>) powder under vacuum to 120 °C and collecting the gaseous monomer in a trap at 77 K. Methylglyoxal, CH<sub>3</sub>COCHO (MGly), was obtained from 40% aqueous solution of methylglyoxal (Sigma-Aldrich). The major amount of water was distilled off in a vacuum line; then, the sample was depolymerized by heating at about 90 °C. Next, the gaseous monomeric methylglyoxal was passed through P<sub>4</sub>O<sub>10</sub> and trapped in 77 K. The sample was stored at liquid nitrogen temperature. Hydroxylamine, NH<sub>2</sub>OH (HA), was generated by heating (at 50–65 °C) the hydroxylamine phosphate salt (95%, Fluka: Buchs, Switzerland) directly in the deposition line. Deuterated hydroxylamine, ND<sub>2</sub>OD (d-HA), was prepared by heating hydroxylamine phosphate salt in D<sub>2</sub>O solution and evaporating water in a vacuum. This procedure was repeated several times until the deuteration degree was about 90%.

The carbonyl/hydroxylamine/argon (or nitrogen) matrices were prepared by simultaneous deposition of carbonyl/Ar(N<sub>2</sub>) and NH<sub>2</sub>OH vapor on a cold gold mirror held at 11–17 K by a closed-cycle helium refrigerator (Displex 202A, Air Products: Allentown, PA, USA). The carbonyl/Ar(N<sub>2</sub>) concentration was varied in a range of 1/100–1/2000. The absolute concentration of NH<sub>2</sub>OH in the matrices could not be determined, but its concentration was varied by changing the rare gas flow rate and the heating temperature of the hydroxylamine salt. The infrared spectra with a resolution of 0.5  $\text{cm}^{-1}$  were recorded in a reflection mode with Bruker 113v FTIR spectrometer using a liquid-nitrogen-cooled MCT detector.

The bands that are assigned to the 1:1 complexes between carbonyl and hydroxylamine were observed already in the spectra of the diluted matrices; their relative intensities with respect to the other species trapped in the matrix decreased after matrix annealing and when the matrix concentration increased. The relative intensities of all bands assigned to one type of the 1:1 complex were constant in all performed experiments. Matrix annealing

increased the concentration of the HA dimers and higher-order complexes and obscured the spectra.

The MP2 method with 6-311++G(2d,2p) basis set was used for geometry optimization of the structures and calculation of harmonic vibrational spectra of the monomers and hydroxylamine (HA- and d-HA-substituted) complexes with FA, Gly and MGly [75,76]. All the presented monomer and complex structures correspond to the real minima on PES as indicated by the positive values of their calculated wavenumbers. Binding energies were corrected by the Boys–Bernardi full counterpoise procedure [77]. The calculations were performed using the Gaussian 03 program [78]. The topological analysis of the electron density was performed with the AIMAll program [79].

#### 4. Conclusions

The FTIR matrix isolation spectroscopy and MP2/6-311++G(2d,2p) calculations were applied to investigate the complexes of formaldehyde and  $\alpha$ -dicarbonyls (glyoxal, methylglyoxal) with hydroxylamine in solid argon and nitrogen matrices. The results of the study show that  $\text{NH}_2\text{OH}$  forms with carbonyls two types of hydrogen-bonded complexes. One type involves the nonplanar structures stabilized by the  $\text{O}-\text{H}\cdots\text{O}(\text{C})$  interactions in which the hydroxylamine moiety is placed above the carbonyl group of formaldehyde or above one of the two  $\text{C}=\text{O}$  groups of  $\alpha$ -dicarbonyls. The ab initio calculations predict this structure as the most stable form of the 1:1 complex between  $\alpha$ -dicarbonyl and hydroxylamine. The other type includes the planar cyclic structure stabilized by the  $\text{O}-\text{H}\cdots\text{O}(\text{C})$  and  $\text{C}-\text{H}\cdots\text{N}$  hydrogen bonds. This structure is predicted to be the most stable one for  $\text{HCHO}-\text{NH}_2\text{OH}$  and was observed for this complex isolated in both argon and nitrogen matrices. The structure of the glyoxal–hydroxylamine complex is affected by the matrix in which it is isolated. In the argon matrix, the most stable nonplanar complex is formed, whereas in solid nitrogen, both the cyclic planar structure, corresponding to one of the local minima and the most stable nonplanar structure, are created. In turn, the methylglyoxal–hydroxylamine complex forms the most stable nonplanar structure in both argon and nitrogen matrices.

The obtained data confirm that the matrix can influence the nature of the isolated complex and can stabilize the less stable structures as it was observed for the  $\text{CHOCHO}-\text{NH}_2\text{OH}$  complex. The formation of the less stable complex in matrices is attributed to the dipole–dipole interactions that dominate at long-range geometries and direct the two approaching submolecules in the matrix to one of the energy minima. It is not excluded that the carbonyl complexes with hydroxylamine are formed in a similar way [80]. This kind of process was observed for the formation of formic acid dimers [81], acetohydroxamic acid [82] and *N*-hydroxyurea dimers [83] or *N,N*-dimethylformamide complexes with water and ammonia in solid argon [84].

**Supplementary Materials:** The following are available online, Figure S1: The optimized structures of the HCHO–NH<sub>2</sub>OH complexes; Figure S2: The optimized structures of the CHOCHO–NH<sub>2</sub>OH complexes; Figure S3: The spectra of the CHOCHO/Ar (a), ND<sub>2</sub>OD/Ar (b) and CHOCHO/ND<sub>2</sub>OD/Ar (c) matrices recorded after matrix deposition at 11 K; Figure S4: The spectra of the CHOCHO/N<sub>2</sub> (a), ND<sub>2</sub>OD/N<sub>2</sub> (b) and CHOCHO/ND<sub>2</sub>OD/N<sub>2</sub> (c) matrices recorded after matrix deposition at 11 K; Figure S5: The optimized structures of the CH<sub>3</sub>COCHO–NH<sub>2</sub>OH complexes; Figure S6: The spectra of the CH<sub>3</sub>COCHO/Ar (a), ND<sub>2</sub>OD/Ar (b) and CH<sub>3</sub>COCHO/ND<sub>2</sub>OD/Ar (c) matrices recorded after matrix deposition at 11 K; Figure S7: The location of the bond (3,-1) and ring (3,1) critical points in the MP2/6-311++G(2d,2p) optimized structures of the HCHO–NH<sub>2</sub>OH complexes; Figure S8: The location of the bond (3,-1) and ring (3,1) critical points in the MP2/6-311++G(2d,2p) optimized structures of the CHOCHO–NH<sub>2</sub>OH complexes; Figure S9: The MP2 optimized structures of the formaldehyde, glyoxal and methylglyoxal complexes with hydroxylamine assigned to the structures isolated in argon matrix; Figure S10: The MP2 optimized structures of the formaldehyde, glyoxal and methylglyoxal complexes with hydroxylamine assigned to the structures isolated in nitrogen matrix; Table S1: Selected geometrical parameters of the hydroxylamine and formaldehyde subunits in their binary complexes; Table S2: Selected geometrical parameters of the hydroxylamine and glyoxal subunits in their binary complexes; Table S3: The comparison of the observed wavenumbers (cm<sup>-1</sup>) and wavenumber shifts ( $\Delta\nu = \nu_{GH} - \nu_M$ ) for the CHOCHO–NH<sub>2</sub>OH (GH) complexes present in the Ar and N<sub>2</sub> matrices with the corresponding calculated values for the complexes I<sub>GH</sub>–IV<sub>GH</sub>; Table S4: The comparison of the observed wavenumbers (cm<sup>-1</sup>) and wavenumber shifts ( $\Delta\nu = \nu_{GH} - \nu_M$ ) for the CHOCHO–ND<sub>2</sub>OD (GH) complexes present in the Ar and N<sub>2</sub> matrices with the corresponding calculated values for the complexes I<sub>GH</sub>–IV<sub>GH</sub>; Table S5: Selected geometrical parameters of the hydroxylamine and methylglyoxal subunits in their binary complexes; Table S6: The comparison of the observed wavenumbers (cm<sup>-1</sup>) and wavenumber shifts ( $\Delta\nu = \nu_{MH} - \nu_M$ ) for the CH<sub>3</sub>COCHO–NH<sub>2</sub>OH (MH) complexes present in the Ar and N<sub>2</sub> matrices with the corresponding calculated values for the complexes I<sub>MHk</sub>–IV<sub>MHk</sub> and I<sub>MHa</sub>–IV<sub>MHa</sub>; Table S7: The comparison of the observed wavenumbers (cm<sup>-1</sup>) and wavenumber shifts ( $\Delta\nu = \nu_{MH} - \nu_M$ ) for the CH<sub>3</sub>COCHO–ND<sub>2</sub>OD (MH) complexes present in the Ar and N<sub>2</sub> matrices with the corresponding calculated values for the complexes I<sub>MHk</sub>–IV<sub>MHk</sub> and I<sub>MHa</sub>–IV<sub>MHa</sub>.

**Author Contributions:** Conceptualization, B.G. and Z.M.; methodology, B.G. and Z.M.; formal analysis, B.G. and M.S.; investigation, B.G. and M.S.; resources, Z.M.; data curation, B.G.; writing—original draft preparation, B.G.; writing—review and editing, B.G., Z.M. and M.S.; visualization, B.G.; supervision, Z.M.; project administration, B.G. and Z.M.; funding acquisition, Z.M. All authors have read and agreed to the published version of the manuscript.

**Funding:** This research received no external funding.

**Institutional Review Board Statement:** Not applicable.

**Informed Consent Statement:** Not applicable.

**Data Availability Statement:** The data presented in this study are available in this article.

**Acknowledgments:** The authors acknowledge the Wrocław Supercomputer Centre (WCSS) for providing computer time and facilities.

**Conflicts of Interest:** The authors declare no conflict of interest.

**Sample Availability:** Samples of the compounds are not available from the authors.

## References

1. Whittle, E.; Dows, D.A.; Pimentel, G.C. Matrix isolation method for the experimental study of unstable species. *J. Chem. Phys.* **1954**, *22*, 1943. [[CrossRef](#)]
2. Ault, B.S. Matrix isolation studies of reactive intermediate complexes. *Rev. Chem. Intermed.* **1988**, *9*, 233–269. [[CrossRef](#)]
3. Barnes, A.J. Matrix isolation studies of hydrogen bonding—An historical perspective. *J. Mol. Struct.* **2018**, *1163*, 77–85. [[CrossRef](#)]
4. Rosenberg, S.; Silver, S.M.; Sayer, J.M.; Jencks, W.P. Evidence for two concurrent mechanisms and a kinetically significant proton transfer process in acid-catalyzed o-methyloxime formation. *J. Am. Chem. Soc.* **1974**, *96*, 7986–7998. [[CrossRef](#)]
5. Sayer, J.M.; Pinsky, B.; Schonbrunn, A.; Washtien, W. Mechanism of carbinolamine formation. *J. Am. Chem. Soc.* **1974**, *96*, 7998–8009. [[CrossRef](#)]

6. Lahann, J. *Click Chemistry for Biotechnology and Materials Science*; John Wiley and Sons Ltd.: Chichester, UK, 2009; ISBN 9780470699706.
7. Gauthier, M.A.; Klok, H.A. Peptide/protein-polymer conjugates: Synthetic strategies and design concepts. *Chem. Commun.* **2008**, 2591–2611. [[CrossRef](#)]
8. Venkatesan, N.; Kim, B.H. Peptide conjugates of oligonucleotides: Synthesis and applications. *Chem. Rev.* **2006**, *106*, 3712–3761. [[CrossRef](#)]
9. Hermanson, G.T. *Bioconjugate Techniques*, 3rd ed.; Elsevier: Amsterdam, The Netherlands, 2013; ISBN 978-0-12-382239-0.
10. Kubler-Kielb, J. Conjugation of LPS-derived oligosaccharides to proteins using oxime chemistry. *Methods Mol. Biol.* **2011**, *751*, 317–327. [[CrossRef](#)] [[PubMed](#)]
11. Kölmel, D.K.; Kool, E.T. Oximes and hydrazones in bioconjugation: Mechanism and catalysis. *Chem. Rev.* **2017**, *117*, 10358–10376. [[CrossRef](#)]
12. Lowry, T.H.; Schueller Richardson, K. *Mechanism and Theory in Organic Chemistry*, 2nd ed.; HarperCollins Publishers: New York, NY, USA, 1987; ISBN 13-978-0063504288.
13. Morokuma, K. Molecular orbital studies of hydrogen bonds. III. C=O...H-O hydrogen bond in H<sub>2</sub>CO...H<sub>2</sub>O and H<sub>2</sub>CO...2H<sub>2</sub>O. *J. Chem. Phys.* **1971**, *55*, 1236–1244. [[CrossRef](#)]
14. Del Bene, J.E. Molecular orbital theory of hydrogen bond. VI. Effect of hydrogen bonding on n-π\* transitions in dimers ROHOCH<sub>2</sub>. *J. Am. Chem. Soc.* **1973**, *2042*, 6517–6522. [[CrossRef](#)]
15. Ventura, O.N.; Coitiño, E.L.; Irving, K.; Iglecias, A.; Lledós, A. Comparison of semiempirical and bsse corrected møller-pleeset ab initio calculations on the direct addition of water to formaldehyde. *J. Mol. Struct. Theochem.* **1990**, *210*, 427–440. [[CrossRef](#)]
16. Vos, R.J.; Hendriks, R.; Van Duijneveldt, F.B. SCF, MP2 and CEPA-1 calculations on the OH-O hydrogen bonded complexes (H<sub>2</sub>O)<sub>2</sub> and (H<sub>2</sub>O-H<sub>2</sub>CO). *J. Comput. Chem.* **1990**, *11*, 1–18. [[CrossRef](#)]
17. Nelander, B. A matrix isolation study of the water-formaldehyde complex. The far-infrared region. *Chem. Phys.* **1992**, *159*, 281–287. [[CrossRef](#)]
18. Ventura, O.N.; Coitiño, E.L.; Lledós, A.; Bertran, J. Analysis of the gas-phase addition of water to formaldehyde: A semiempirical and ab initio study of bifunctional catalysis by H<sub>2</sub>O. *J. Comput. Chem.* **1992**, *13*, 1037–1046. [[CrossRef](#)]
19. Ha, T.K.; Makarewicz, J.; Bauder, A. Ab initio study of the water-formaldehyde complex. *J. Phys. Chem.* **1993**, *97*, 11415–11419. [[CrossRef](#)]
20. Dimitrova, Y.; Peyerimhoff, S.D. Theoretical study of the n → π\* transitions in hydrogen-bonded formaldehyde complexes. *Chem. Phys. Lett.* **1994**, *227*, 384–389. [[CrossRef](#)]
21. Sánchez, M.L.; Aguilar, M.A.; Del Valle, F.J.O. Solvent effects on optical emission and absorption spectra: Theoretical calculation of the <sup>1</sup>(n, π\*) transition of formaldehyde in solution. *J. Phys. Chem.* **1995**, *99*, 15758–15764. [[CrossRef](#)]
22. Dimitrova, Y. Solvent effects on vibrational spectra of hydrogen-bonded complexes of formaldehyde and water: An ab initio study. *J. Mol. Struct. Theochem.* **1997**, *391*, 251–257. [[CrossRef](#)]
23. Galano, A.; Narciso-Lopez, M.; Francisco-Marquez, M. Water complexes of important air pollutants: Geometries, complexation energies, concentrations, infrared spectra, and intrinsic reactivity. *J. Phys. Chem. A* **2010**, *114*, 5796–5809. [[CrossRef](#)]
24. Ahlström, M.; Jönsson, B.; Karlström, G. Ab initio molecular orbital calculations on hydrogen- and non-hydrogen-bonded complexes. H<sub>2</sub>CO-H<sub>2</sub>O and H<sub>2</sub>CO-H<sub>2</sub>S. *Mol. Phys* **1979**, 1051–1059. [[CrossRef](#)]
25. Nelander, B. Infrared spectrum of the water formaldehyde complex in solid argon and solid nitrogen. *J. Chem. Phys.* **1980**, *72*, 77–84. [[CrossRef](#)]
26. Butler, L.G.; Brown, T.L. Nuclear quadrupole coupling constants and hydrogen-bonding. A molecular-orbital study of O<sup>17</sup> and deuterium field gradients in formaldehyde-water hydrogen bonding. *J. Am. Chem. Soc.* **1981**, *103*, 6541–6549. [[CrossRef](#)]
27. Williams, I.H.; Spangler, D.; Femec, D.A.; Maggiora, G.M.; Schowen, R.L. Theoretical models for solvation and catalysis in carbonyl addition. *J. Am. Chem. Soc.* **1983**, *105*, 31–40. [[CrossRef](#)]
28. Lewell, X.Q.; Hillier, I.H.; Field, M.J.; Morris, J.J.; Taylor, P.J. Theoretical studies of vibrational frequency shifts upon hydrogen bonding. The carbonyl stretching mode in complexes of formaldehyde. *J. Chem. Soc. Faraday Trans. 2* **1988**, *84*, 893–898. [[CrossRef](#)]
29. Blair, J.T.; Krogh-Jespersen, K.; Levy, R.M. Solvent effects on optical absorption spectra: The <sup>1</sup>A<sub>1</sub>—<sup>1</sup>A<sub>2</sub> transition of formaldehyde in water. *J. Am. Chem. Soc.* **1989**, *111*, 6948–6956. [[CrossRef](#)]
30. Blair, J.T.; Westbrook, J.D.; Levy, R.M.; Kroghjespersen, K. Simple-models for solvation effects on electronic-transition energies. Formaldehyde and water. *Chem. Phys. Lett.* **1989**, *154*, 531–535. [[CrossRef](#)]
31. Kumpf, R.A.; Damewood, J.R. Interaction of formaldehyde with water. *J. Phys. Chem.* **1989**, *93*, 4478–4486. [[CrossRef](#)]
32. Nelander, B. Infrared spectra of formaldehyde complexes with hydrogen bromide, chlorine and iodine chloride. *J. Mol. Struct.* **1980**, *69*, 59–68. [[CrossRef](#)]
33. Nelander, B. Infrared spectra and structure of formaldehyde complexes with ammonia and acetonitrile. *J. Mol. Struct.* **1982**, *81*, 223–228. [[CrossRef](#)]
34. Baiocchi, F.A.; Klemperer, W. The rotational and hyperfine spectrum and structure of H<sub>2</sub>CO-HF. *J. Chem. Phys.* **1983**, *78*, 3509–3520. [[CrossRef](#)]
35. Bach, S.B.H.; Ault, B.S. Infrared matrix isolation study of the hydrogen-bonded complexes between formaldehyde and the hydrogen halides and cyanide. *J. Phys. Chem.* **1984**, *88*, 3600–3604. [[CrossRef](#)]
36. Rivelino, R. Lewis acid-base interactions in weakly bound formaldehyde complexes with CO<sub>2</sub>, HCN, and FCN: Considerations on the cooperative H-bonding effects. *J. Phys. Chem. A* **2008**, *112*, 161–165. [[CrossRef](#)]

37. Mitchell, J.B.O.; Price, S.L. The nature of the N-H O-C hydrogen bond—An intermolecular perturbation theory study of the formamide/formaldehyde complex. *J. Comput. Chem.* **1990**, *11*, 1217–1233. [[CrossRef](#)]
38. Tolosa, S.; Hidalgo, A.; Sansón, J.A. Thermodynamic, structural, and dynamic study of the N-H···O=C hydrogen bond association in aqueous solution. *Chem. Phys.* **2000**, *255*, 73–84. [[CrossRef](#)]
39. Müller, R.P.; Russegger, P.; Huber, J.R. Hydrogen-bonded complex between HNO and formaldehyde. Photolysis of methyl nitrite in an argon matrix. *Chem. Phys.* **1982**, *70*, 281–290. [[CrossRef](#)]
40. Moore, K.B.; Sadeghian, K.; Sherrill, C.D.; Ochsenfeld, C.; Schaefer, H.F. C-H···O Hydrogen bonding. the prototypical methane-formaldehyde system: A critical assessment. *J. Chem. Theory Comput.* **2017**, *13*, 5379–5395. [[CrossRef](#)]
41. Brumer, Y.; Shapiro, M.; Brumer, P.; Baldrige, K.K. Controlled alcohol-ketone interconversion by dihydrogen transfer: An ab initio study of the methanol-formaldehyde complex. *J. Phys. Chem. A* **2002**, *106*, 9512–9519. [[CrossRef](#)]
42. Mucha, M.; Mielke, Z. Complexes of atmospheric  $\alpha$ -dicarbonyls with water: FTIR Matrix isolation and theoretical study. *J. Phys. Chem. A* **2007**, *111*, 2398–2406. [[CrossRef](#)]
43. Mielke, Z.; Mucha, M.; Bil, A.; Golec, B.; Coussan, S.; Roubin, P. Photo-induced hydrogen exchange reaction between methanol and glyoxal: Formation of hydroxyketene. *ChemPhysChem* **2008**, *9*, 1774–1780. [[CrossRef](#)]
44. Mucha, M.; Mielke, Z. Structure and photochemistry of the methanol complexes with methylglyoxal and diacetyl: FTIR matrix isolation and theoretical study. *Chem. Phys.* **2009**, *361*, 27–34. [[CrossRef](#)]
45. Mucha, M.; Mielke, Z. Photochemistry of the glyoxal-hydrogen peroxide complexes in solid argon: Formation of 2-hydroxy-2-hydroperoxyethanal. *Chem. Phys. Lett.* **2009**, *482*, 87–92. [[CrossRef](#)]
46. Mucha, M. Faculty of Chemistry. Ph.D. Thesis, University of Wrocław, Wrocław, Poland, 2008.
47. Aloisio, S.; Francisco, J.S. Complexes of hydroperoxyl radical with glyoxal, methylglyoxal, methylvinyl ketone, acrolein, and methacrolein: Possible new sinks for HO<sub>2</sub> in the atmosphere? *J. Phys. Chem. A* **2003**, *107*, 2492–2496. [[CrossRef](#)]
48. Yeo, G.A.; Ford, T.A. The infrared spectrum of the hydroxylamine dimer. *J. Mol. Struct.* **1990**, *217*, 307–323. [[CrossRef](#)]
49. Yeo, G.A.; Ford, T.A. Matrix isolation infrared spectrum of the water-hydroxylamine complex. *Vib. Spectrosc.* **1991**, *253*, 173–181. [[CrossRef](#)]
50. Yeo, G.A.; Ford, T.A. The matrix isolation infrared spectrum of the hydroxylamine-ammonia complex. *Spectrochim. Acta Part A* **1991**, *47*, 919–925. [[CrossRef](#)]
51. Sałdyka, M.; Mielke, Z. Photodecomposition of formohydroxamic acid. Matrix isolation FTIR and DFT studies. *Phys. Chem. Chem. Phys.* **2003**, *5*, 4790–4797. [[CrossRef](#)]
52. Sałdyka, M. Photodecomposition of N-hydroxyurea in argon matrices. FTIR and theoretical studies. *RSC Adv.* **2013**, *3*, 1922–1932. [[CrossRef](#)]
53. Khoshkhoo, H.; Nixon, E.R. Infrared and Raman spectra of formaldehyde in argon and nitrogen matrices. *Spectrochim. Acta Part A* **1973**, *29*, 603–612. [[CrossRef](#)]
54. Nelander, B. Infrared spectrum of formaldehyde in solid nitrogen. I. Monomer absorption. *J. Chem. Phys.* **1980**, *73*, 1026–1033. [[CrossRef](#)]
55. Nelander, B. Infrared spectrum of formaldehyde in solid nitrogen. II. Dimer spectrum and dimer structure. *J. Chem. Phys.* **1980**, *73*, 1034–1039. [[CrossRef](#)]
56. Withnall, R.; Andrews, L. Matrix infrared spectra and normal-coordinate analysis of isotopic hydroxylamine molecules. *J. Phys. Chem.* **1988**, *92*, 2155–2161. [[CrossRef](#)]
57. Kuchtsu, K.; Fukuyama, T.; Morino, Y. Average structures of butadiene, acrolein, and glyoxal determined by gas electron diffraction and spectroscopy. *J. Mol. Struct.* **1968**, *1*, 463–479. [[CrossRef](#)]
58. Osamura, Y.; Schaefer, H.F. Internal rotation barrier and transition state for glyoxal. *J. Chem. Phys.* **1981**, *74*, 4576–4580. [[CrossRef](#)]
59. Diem, M.; MacDonald, B.G.; Lee, E.K.C. Photolysis and laser-excited fluorescence and phosphorescence emission of trans-glyoxal in an argon matrix at 13 K. *J. Phys. Chem.* **1981**, *85*, 2227–2232. [[CrossRef](#)]
60. Profeta, L.T.M.; Sams, R.L.; Johnson, T.J.; Williams, S.D. Quantitative infrared intensity studies of vapor-phase glyoxal, methylglyoxal, and 2,3-butanedione (diacetyl) with vibrational assignments. *J. Phys. Chem. A* **2011**, *115*, 9886–9900. [[CrossRef](#)]
61. Hobza, P.; Havlas, Z. Blue-shifting hydrogen bonds. *Chem. Rev.* **2000**, *100*, 4253–4264. [[CrossRef](#)]
62. Hermansson, K. Blue-shifting hydrogen bonds. *J. Phys. Chem. A* **2002**, *106*, 4695–4702. [[CrossRef](#)]
63. Karpfen, A.; Kryachko, E.S. Blue-shifted hydrogen-bonded complexes. II. CH<sub>3</sub>F···(HF)<sub>1≤n≤3</sub> and CH<sub>2</sub>F<sub>2</sub>···(HF)<sub>1≤n≤3</sub>. *Chem. Phys.* **2005**, *310*, 77–84. [[CrossRef](#)]
64. Rutkowski, K.S.; Rodziewicz, P.; Melikova, S.M.; Koll, A. Theoretical study of Hal<sub>3</sub>CH/F<sub>2</sub>CD<sub>2</sub> (Hal=F,Cl) and F<sub>3</sub>CH/FH heterodimers with blue shifted hydrogen bonds. *Chem. Phys.* **2006**, *327*, 193–201. [[CrossRef](#)]
65. Melikova, S.M.; Rutkowski, K.S.; Rodziewicz, P.; Koll, A. Unusual spectroscopic properties of CF<sub>3</sub>H dissolved in liquified Ar, N<sub>2</sub>, CO and CO<sub>2</sub>. *Chem. Phys. Lett.* **2002**, *352*, 301–310. [[CrossRef](#)]
66. Asfin, R.E.; Melikova, S.M.; Rutkowski, K.S. The infrared study of fluoroform+methyl fluoride mixtures in argon and nitrogen matrices. Evidence of nonlinear blue-shifting complex formation. *Spectrochim. Acta Part A* **2018**, *208*, 185–194. [[CrossRef](#)]
67. Dyllick-Brenzinger, C.E.; Bauder, A. Microwave spectrum, dipole moment and barrier to internal rotation of trans-methyl glyoxal. *Chem. Phys.* **1978**, *30*, 147–153. [[CrossRef](#)]
68. Reid, S.A.; Kim, H.L.; McDonald, J.D. A stimulated emission pumping study of jet-cooled methyl glyoxal. *J. Chem. Phys.* **1990**, *92*, 7079–7086. [[CrossRef](#)]

69. Grabowski, S.J. What is the covalency of the hydrogen bonding? *Chem. Rev.* **2011**, *111*, 2597–2625. [[CrossRef](#)] [[PubMed](#)]
70. Koch, U.; Popelier, P.L.A. Characterization of C-H-O hydrogen-bonds on the basis of the charge density. *J. Phys. Chem.* **1995**, *99*, 9747–9754. [[CrossRef](#)]
71. Kraka, E.; Zou, W.; Tao, Y. Decoding chemical information from vibrational spectroscopy data: Local vibrational mode theory. *WIREs Comput. Mol. Sci.* **2020**, *10*, e1480. [[CrossRef](#)]
72. Kalescky, R.; Zou, W.; Kraka, E.; Cremer, D. Local vibrational modes of the water dimer—Comparison of theory and experiment. *Chem. Phys. Lett.* **2012**, *554*, 243–247. [[CrossRef](#)]
73. Tao, Y.; Zou, W.; Jia, J.; Li, W.; Cremer, D. Different ways of hydrogen bonding in water—Why does warm water freeze faster than cold water? *J. Chem. Theory Comput.* **2017**, *13*, 55–76. [[CrossRef](#)]
74. Tao, Y.; Zou, W.; Kraka, E. Strengthening of hydrogen bonding with the push-pull effect. *Chem. Phys. Lett.* **2017**, *685*, 251–258. [[CrossRef](#)]
75. Frisch, M.J.; Pople, J.A.; Binkley, J.S. Self-consistent molecular orbital methods 25. Supplementary functions for Gaussian basis sets. *J. Chem. Phys.* **1984**, *80*, 3265–3269. [[CrossRef](#)]
76. Krishnan, R.; Binkley, J.S.; Seeger, R.; Pople, J.A. Self-consistent molecular orbital methods. XX. A basis set for correlated wave functions. *J. Chem. Phys.* **1980**, *72*, 650–654. [[CrossRef](#)]
77. Boys, S.F.; Bernardi, F. Calculation of small molecular interactions by differences of separate total energies—Some procedures with reduced errors. *Mol. Phys.* **1970**, *19*, 553–566. [[CrossRef](#)]
78. Frisch, M.J.; Trucks, G.W.; Schlegel, H.B.; Scuseria, G.E.; Robb, M.A.; Cheeseman, J.R.; Montgomery, J.A., Jr.; Vreven, T.; Kudin, K.N.; Burant, J.C.; et al. *Gaussian 03, Revision, C.02*; Gaussian Inc.: Wallingford, CT, USA, 2003.
79. Keith, T.A. AIMAll, Version 12.09.23, Standard, 1997–2012. Available online: <http://aim.tkgristmill.com> (accessed on 19 February 2021).
80. Barnes, A.J.; Mielke, Z. Matrix effects on hydrogen-bonded complexes trapped in low-temperature matrices. *J. Mol. Struct.* **2012**, *1023*, 216–221. [[CrossRef](#)]
81. Gantenberg, M.; Halupka, M.; Sander, W. Dimerization of formic acid—an example of a “noncovalent” reaction mechanism. *Chem. Eur. J.* **2000**, *6*, 1865–1869. [[CrossRef](#)]
82. Sałdyka, M.; Mielke, Z. Dimerization of the keto tautomer of acetohydroxamic acid—Infrared matrix isolation and theoretical study. *Spectrochim. Acta A Mol. Biomol. Spectrosc.* **2005**, *61*, 1491–1497. [[CrossRef](#)] [[PubMed](#)]
83. Sałdyka, M. N-Hydroxyurea dimers: A matrix isolation and theoretical study. *Vib. Spectrosc.* **2016**, *85*, 149–156. [[CrossRef](#)]
84. Sałdyka, M.; Mielke, Z.; Haupa, K. Structural and spectroscopic characterization of DMF complexes with nitrogen, carbon dioxide, ammonia and water. Infrared matrix isolation and theoretical studies. *Spectrochim. Acta A Mol. Biomol. Spectrosc.* **2018**, *190*, 423–432. [[CrossRef](#)]